Intracellular localization of diffusible elements in frozen-hydrated specimens with ion microscopy

ARTICLE *in* ANALYTICAL CHEMISTRY · MARCH 1986

Impact Factor: 5.64 · DOI: 10.1021/ac00293a053 · Source: PubMed

3 AUTHORS, INCLUDING:

Subhash Chandra
Cornell University
78 PUBLICATIONS **1,688** CITATIONS

SEE PROFILE

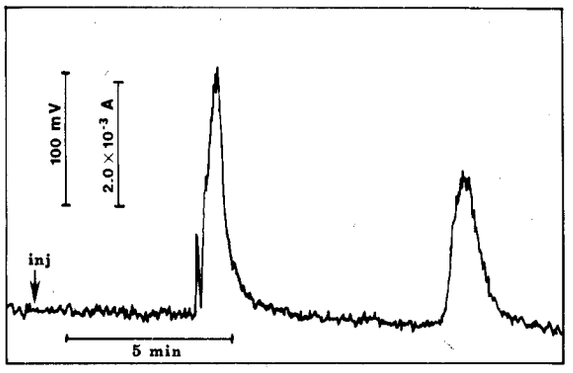

Figure 3. Photoacoustic detection of azulene in supercritical CO_2, elution of 20-μL injected sample of azulene 6.26 × 10^{-4} M (second peak) in methanol (first peak).

with the photoacoustic sensitivity comparison of nonpolar and polar liquids above, the decrease in the speed of sound in supercritical fluids moderates the effect of the expansion coefficient and limits the overall increase in sensitivity. Since the speed of sound and expansion coefficient both depend on the degree of intermolecular interaction in the fluid, they tend to change inversely to one another as the fluid is taken from liquid to dense gas conditions (*28–30*). As a result, the sensitivity of photoacoustic detection is not as strongly affected as thermooptical detection methods by the approach to the critical point of the solvent.

The observed photoacoustic sensitivity in supercritical CO_2 near its critical point is nearly an order of magnitude greater than CCl_4, the best liquid solvent tested. While this increase in sensitivity is not as large as that encountered with thermal lens measurements, the result could, nevertheless, provide a significant benefit for photoacoustic detection in supercritical fluid chromatography, for example. Flowing the sample for photoacoustic measurements does not reduce the sensitivity of detection as observed with the thermal lens method (*32*). Furthermore, the high frequency, band-pass filter on the preamplifier eliminates the low-frequency acoustic noise associated with the flowing sample.

Although the experiments in this study were designed primarily to test the relative sensitivity of photoacoustic detection in supercritical fluids, they also provide an opportunity to evaluate noise contributions. The predominant source of background noise was found to be from scattered laser radiation striking the walls of the stainless steel flow cell. The small internal diameter of the flow cell precluded time resolving this background from sound generated within the solvent. Absorption detection limits in CO_2, estimated from the base line noise as in Figure 1, were not outstanding, $A_{min} = 1.4 \times 10^{-4}$. Since the major source of stray light within the cell was reflections and scatter from the sapphire windows, one might improve on these results by using antireflection-coated windows with a higher quality surface polish. Absorption of the stray light by the cell walls might also be reduced by coating the surfaces with a material that is more reflective than stainless steel or by construction of the cell using entirely dielectric materials. These modifications could reduce the background noise level by more than an order of magnitude.

Registry No. CO_2, 124-38-9; azulene, 275-51-4; methylene blue, 61-73-4; solvent green 3, 128-80-3.

LITERATURE CITED

(1) Patel, C. K. N.; Tam, A. C. *Appl. Phys. Lett.* **1979**, *34*, 467–470.
(2) Oda, S.; Sawada, T. *Anal. Chem.* **1981**, *53*, 471–474.
(3) Voigtman, E.; Jurgensen, A.; Winefordner, J. *Anal. Chem.* **1981**, *53*, 1442–1446.
(4) Hu, C.; Whinnery, J. R. *Appl. Opt.* **1973**, *12*, 72–79.
(5) Hordvik, A. *Appl. Opt.* **1977**, *16*, 2827–2833.
(6) Dovichi, N. J.; Harris, J. M. *Anal. Chem.* **1979**, *51*, 728–731.
(7) Tam, A. C.; Patel, C. K. N. *Appl. Opt.* **1979**, *18*, 3348–3357.
(8) Patel, C. K. N.; Tam, A. C. *Rev. Mod. Phys.* **1981**, *53*, 517–550.
(9) Kiesper, E.; Corwin, A. H.; Turner, D. A. *J. Org. Chem.* **1962**, *27*, 700–701.
(10) Giddings, J. C.; Manwaring, W. A.; Myers, M. N. *Science* **1966**, *154*, 146–150.
(11) Novotny, M.; Springston, S. R.; Peaden, P. A.; Fjeldsted, J. C.; Lee, M. L. *Anal. Chem.* **1981**, *53*, 407A–414A.
(12) Gere, D. R. *Science* **1983**, *222*, 253–259.
(13) Shafer, K. H.; Griffiths, P. R. *Anal. Chem.* **1983**, *55*, 1939–1942.
(14) Leach, R. A.; Harris, J. M. *Anal. Chem.* **1984**, *56*, 1481–1487.
(15) Leach, R. A.; Harris, J. M. *Anal. Chem.* **1984**, *56*, 2801–2805.
(16) Hordvik, A.; Schlossberg, H. *Appl. Opt.* **1977**, *16*, 101–107.
(17) Farrow, M. M.; Burnham, R. K.; Auzanneau, M.; Olsen, S. L.; Purdie, N.; Eyring, E. M. *Appl. Opt.* **1978**, *17*, 1093–1098.
(18) Tam, A. C.; Patel, C. K. N.; Kerl, R. J. *Opt. Lett.* **1979**, *4*, 81–83.
(19) Parker, C. A. "Photoluminescence of Solutions"; Academic: New York, 1968.
(20) Melhuish, W. H. *NBS Spec. Publ. (U.S.)* **1973**, *No. 378*, 137–150.
(21) Brannon, J. H.; Magde, D. *J. Phys. Chem.* **1978**, *82*, 705–709.
(22) Harrison, D.; Moelwyn-Hughes, E. A. *Proc. R. Soc. London, A* **1957**, *239*, 230.
(23) Bolz, R. E., Tuve, G. L., Eds. "Handbook of Tables for Applied Engineering Science"; CRC Press: Cleveland, OH, 1973; pp 88, 92.
(24) Weast, R. C., Ed. "Handbook of Chemistry and Physics", 57th ed.; **1977**, CRC Press: Cleveland, OH, 1977; p E-47.
(25) Washburn, E. W., Ed. "International Critical Tables"; McGraw-Hill: New York, 1930; Vol. 3; pp 25–28.
(26) Mori, K.; Imasaka, T.; Ishibashi, N. *Anal. Chem.* **1982**, *54*, 2034–2038.
(27) Birks, J. B. "Photophysics of Aromatic Molecules"; Wiley: London, 1970, Chapter 5.
(28) Michaels, A.; Hamers, J. *Physica (Amsterdam)* **1937**, *10*, 995–1006.
(29) Michels, A.; Blaisse, B.; Michels, C. *Proc. R. Soc. London, A* **1937**, *160*, 358–375.
(30) Herget, C. M. *J. Chem. Phys.* **1940**, *8*, 537–542.
(31) Burden, R. L.; Faires, J. D.; Reynolds, A. C. "Numerical Analysis"; 2nd ed.; Prindle, Weber and Schmidt: Boston, MA, 1981; pp 107–123.
(32) Dovichi, N. J.; Harris, J. M. *Anal. Chem.* **1981**, *53*, 689–692.

[1] Present address: Corporate Research Sciences Laboratories, Exxon Research and Engineering Company, Clinton Township, Route 22 East, Annandale, NJ 08801.
[2] Present address: E 302/126, Du Pont Experimental Station, Wilmington, DE 19898.

F. D. Hardcastle[1]
R. A. Leach[2]
J. M. Harris*

Department of Chemistry
University of Utah
Salt Lake City, Utah 84112

RECEIVED for review August 16, 1985. Accepted October 7, 1985. This research was sponsored in part by the National Science Foundation under Grants CHE 82-06898 and CHE 85-06667 and by fellowship support to J.M.H. from the Alfred P. Sloan Foundation.

Intracellular Localization of Diffusible Elements in Frozen-Hydrated Biological Specimens with Ion Microscopy

Sir: Diffusible elements such as K, Na, and Ca play vital roles in biological processes, and their cytochemical localization has become a major area of research. Ion microscopy, based on secondary ion mass spectrometry (SIMS), provides a

0003-2700/86/0358-0493$01.50/0

powerful technique for such studies. The unique ion optics of the instrument are capable of producing ion images with cell morphology with ~0.5 μm spatial resolution (*1*, *2*). Since the technique is based on mass spectrometry, an unambiguous multielemental (isotopic) distribution can be studied from the same cells. The high sensitivity of the technique in detecting parts-per-million quantities of elements is well suited in studying the role of physiologically important low concentration elements such as Ca in biological systems. Due to the requirements of the instrument, the samples have to be fixed and mounted on a conducting substrate since the sample is held at ±4500 V. The fixation of samples before analysis introduces the classical sample preparation problem in elemental microscopy.

The hydrated biological matrix and the highly diffusible nature of cations (Na^+, K^+, Ca^+, etc.) and their asymmetric distribution between inside and outside the cell pose important challenges for a reliable fixation. An ideal sample preparation methodology should preserve the morphological and chemical state of a living cell and, in addition, should also satisfy the sample requirements of the instrument used to study these parameters. Conventional methods of biological sample preparation for ion microscopy, such as fixation using chemical fixatives followed by dehydration with organic solvents and finally embedment in plastic resins, suffer from artifactual relocation and loss of diffusible elements from their native states (*3*, *4*). Freeze-substitution followed by plastic embedment may offer a better retention but intracellular relocation of diffusible ions cannot be overruled (*5*). Recently, cryotechniques have been recognized to be the only means of a reliable sample fixation methodology before ion microanalysis. Cryofixation followed by freeze-drying can be used in the absence of a cold stage in the instrument; however, reliability of the freeze-drying process has to be confirmed in every study. A cold stage in the instrument would allow a direct analysis of frozen-hydrated specimens, thereby limiting the artifacts caused by preparatory steps other than freezing.

The recently developed liquid nitrogen cooled cold stage for the CAMECA IMS-3f ion microscope (*6*) offers the opportunity to study the distribution of diffusible elements in frozen-hydrated biological specimens. This is the first study in ion microscopy to explore the potential of the technique in analyzing frozen-hydrated soft biological tissue and cultured cells at temperatures below −180 °C. Reliable means of transferring frozen-hydrated samples to the instrument are also described in this paper.

EXPERIMENTAL SECTION

Samples. Cultures of 3T3 mouse fibroblasts maintained in Dulbecco's modified Eagles medium with 10% fetal calf serum (Gibco) and cryosections of chick intestine were used as model systems for this study.

3T3 cells were grown directly on semiconductor grade silicon wafer pieces (General Diode) since an electrically conducting substrate is a necessity for ion microscopy. The nontoxicity of this substrate and its ability to allow comparable cell growth rate and morphologies to cells grown on glass coverslips have been evaluated for a number of cell lines (*7*, *8*). The cells were seeded at a density of 3.0×10^5 per 100-mm Falcon plastic petri dish and incubated at 37 °C in a 5% CO_2 atmosphere. The petri dish contained a few silicon wafer pieces approximmtely 1 cm^2 in size. The cells were grown on the polished side of silicon wafers that allowed visual examinations with a reflected light microscope. Upon confluency in about 4 days, 3T3 cells were freeze-fixed in liquid nitrogen slush and cryofractured using a sandwich-fracture technique under liquid nitrogen (*7*, *9*). The frozen-hydrated cells were kept under liquid nitrogen before ion microanalysis. This sandwich fracture technique has been successfully used in ion microscopy to image the intracellular elemental distribution and ouabain induced Na^+/K^+ ion transport in freeze-dried cultured cells (*8*).

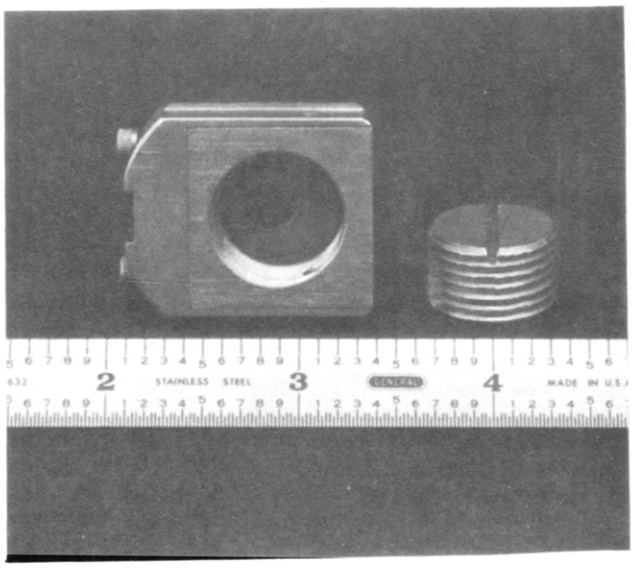

Figure 1. Cryogenic sample holder for Cameca IMS-3f ion microscope.

Cryosections (approximately 2 μm thick) of chick intestine were obtained at −30 °C. The higher sectioning temperature was chosen due to its feasibility in producing thick sections. The thicker sections were preferred because of their ease in handling and pressing the sections on to precooled silicon wafers. The possibility of damaging the morphology to a certain extent in this unavoidable step cannot be ignored. The silicon wafers containing sections were stored in liquid nitrogen until analyzed.

Sample Transfer System. A sample transfer system is necessary for transferring the frozen-hydrated samples to the instrument's precooled sample stage in a frozen-hydrated state. Any substantial rise in temperature of the frozen-hydrated samples at this stage is conducive to the production of artifacts. A new cryogenic sample holder was designed for CAMECA IMS-3f ion microscope to serve the additional function of a transfer mechanism system. The cryogenic sample holder is comprised of a copper block and a copper bolt, rather than the spring-loaded open design of the standard Cameca sample holder (Figure 1). The copper block serves as a thermal reservoir during sample transfer and the copper bolt provides a thermally conducting backing to the sample situated on the silicon substrate. The silicon wafer is held in place by the aforementioned copper bolt. The copper block is situated inside a stainless steel frame of low thermal conductivity, machined identical with the standard sample holder. This frame provides an effective thermal barrier when used with the standard sample transfer arm, which must come in contact with it. The copper is gold plated to assist in the ease of assembly under liquid nitrogen, where the frozen-hydrated sample is mounted in place.

In order to transfer the frozen-hydrated samples to the cryogenic sample holder, the sample holder assembly was precooled to liquid nitrogen temperature by placing it in a liquid-nitrogen-filled Styrofoam container. The silicon wafer containing the frozen-hydrated sample was then transferred under liquid nitrogen and gently mounted in the sample holder. The copper bolt was tightened under liquid nitrogen to hold the silicon wafer in place. The sample holder was then removed from the liquid nitrogen in a dry atmosphere of N_2 and quickly inserted into the air lock of the sample chamber assembly of the ion microscope. In approximately 30 s the air lock pumped down to allow the transfer of the sample holder to the precooled (<−180 °C) sample stage in the high vacuum environment (~10^{-8} torr) of the instrument's sample chamber. Approximately 1 min of time thus spent inserting the sample holder and pumping down the air lock was considered as a suspect in raising the sample temperature to the undesirable range. This temperature rise was evaluated outside the instrument by mounting a temperature sensor on the silicon wafer. It was observed that within this time the temperature rose from −195 to −190 °C, indicating no substantial rise in the specimen temperature during this operation. In addition, sur-

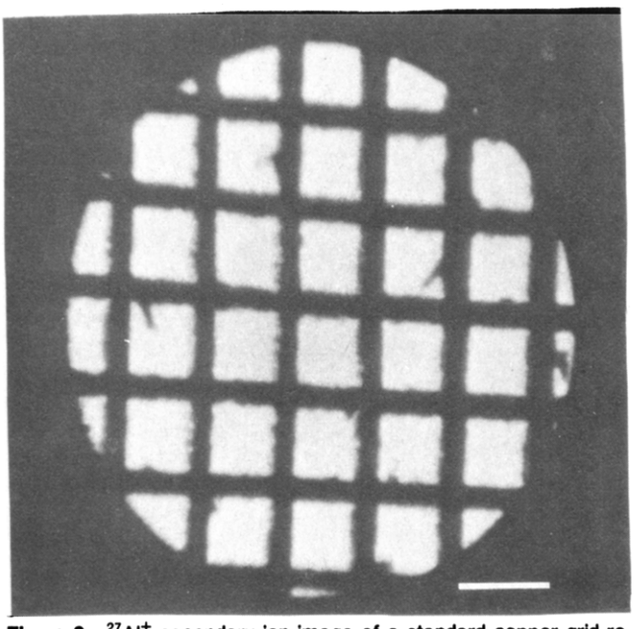

Figure 2. $^{27}Al^+$ secondary ion image of a standard copper grid recorded at −182 °C. Bar = 25 μm.

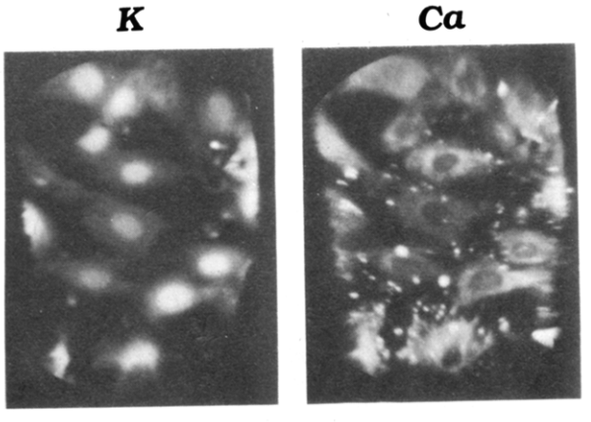

Figure 3. Intracellular distribution of K and Ca in frozen-hydrated 3T3 cells. The presence of brighter spots outside cells in the $^{40}Ca^+$ image is perhaps due to calcium precipitates contributed from the nutrient medium. The circular field aperature, normally used to limit the field of view, was removed from these images. Image exposure times were as follows: K, $^1/_2$ s; Ca, 100 s. Bar = 60 μM.

rounding the air lock with a plastic bag in a dry nitrogen atmosphere substantially reduced atmospheric condensation.

Ion Microscopy. A CAMECA IMS-3f ion microscope/microprobe operating with an 8.0-keV O_2^+ primary ion beam and monitoring positive secondary ions was used for the study. A 200-nA primary beam (~125 μm in diameter) was rastered over an area of 250 × 250 μm^2. The sample stage was precooled to −182 °C before analysis.

RESULTS AND DISCUSSION

Before frozen-hydrated specimens were analyzed, the cryogenic sample holder was evaluated for its normal operation at −182 °C using a standard copper grid mounted on an aluminum substrate. Figure 2 shows the Al^+ (mass 27) secondary ion image indicating no obvious distortion in the secondary optics of the instrument. Good contrast and resolution are clearly evident.

The subcellular distribution of K and Ca in frozen-hydrated and cryofractured 3T3 cells is shown in Figure 3. The nuclei show higher K intensities than the cytoplasm; however for Ca, higher cytoplasmic intensities are observed, and the cytoplasmic Ca does not seem to be homogenously distributed. These observations can be confirmed for each cell in this field of view. No noticeable preferential sputtering of either nuclei or cytoplasm was observed during analysis.

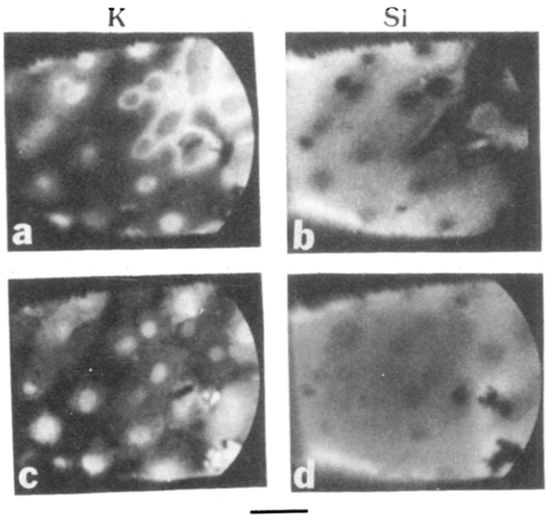

Figure 4. Typical image evolution in frozen-hydrated 3T3 cells revealing the requirement of presputtering before clear morphological details are recognized. Image exposure times were as follows: K, $^1/_2$ s; Si, 1 s. Bar = 60 μM.

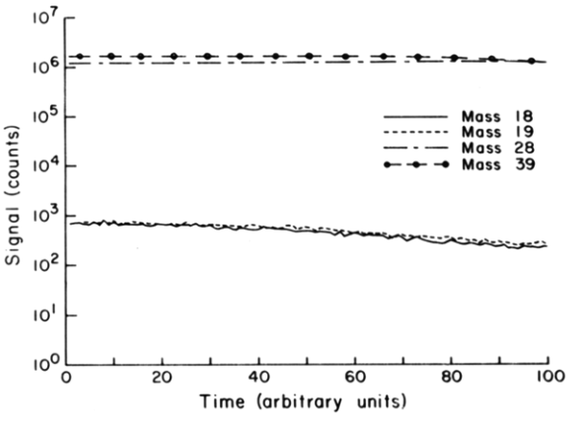

Figure 5. In-depth profile of water at mass 18 and 19 representing H_2O^+ and H_3O^+, respectively, along with K and substrate signals (Si) from 3T3 cells.

Initial charging of the specimen was observed to be the main obstacle in analyzing frozen-hydrated specimens. In order to achieve the image quality shown in Figure 3, presputtering of the samples was generally required. A typical image evolution pattern in frozen-hydrated cells is shown in Figure 4. The field of view contains cells that have been sputtered for different time periods. The left side of the $^{39}K^+$ secondary ion image (Figure 4a) mainly contains cells that were sputtered for about 6 min, and the top right corner contains cells that was sputtered for 2 min. It is evident that cells on the left side show clear morphological details. The substrate image ($^{28}Si^+$) taken immediately after image 4a reveals that the cells showing morphology are thinner as compared to other cells due to longer sputtering (Figure 4b). Figure 4 parts c and d, show $^{39}K^+$ and $^{28}Si^+$ images recorded again from the same field of view after approximately 4 min of additional continuous sputtering. The cells in the top right corner now reveal clear morphological details and seem closer to the substrate. A depth-profile (Figure 5) monitoring water at mass 18 (H_2O^+) and 19 (H_3O^+) along with K and substrate signals from the cells as shown in Figure 4c reveals the presence of water and

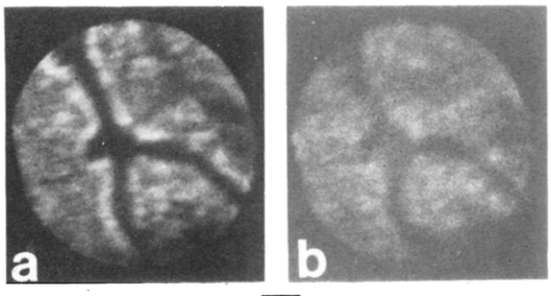

Figure 6. Distribution of Na (a) and water at mass 18 (b) in frozen-hydrated chick intestine section. Image exposure times were as follows: Na, 5 s; H_2O^+, 150 s. Bar = 25 μm.

a slight decline in the water signal with time.

The presputtering requirement was not limited to cultured cells alone. The tissue sections showed the same pattern. The distribution of Na from the frozen-hydrated chick intestine section after approximately 5 min of presputtering is shown in Figure 6a. The brush border shows slightly higher intensities. The K distribution paralleled that of Na. From this field of view an image of water (H_2O^+) was also recorded at mass 18 (Figure 6b). Unlike the Na distribution, no higher intensities of water are observed from brush border. Intervillus spaces seem devoid of elements. It is plausible that intralumenal fluid in these regions sputtered faster due to lack of cellular matrix in these regions. It should be noted that freeze-drying of specimen under the instrumental parameters used is least likely.

The initial charging observed in the frozen-hydrated samples is perhaps due to the buildup of some frost during sample transfer and the frozen water in the specimen since no such charging was observed for freeze-dried samples of the same thickness. It is anticipated that presputtering of the frozen-hydrated samples reduces its thickness to the level that the presence of frozen water in the sample does not interfere with its conductivity. Thin cryo-sections (<0.5 μm), although more vulnerable to ion bombardment, may reduce the presputtering requirement to a certain extent.

It is interesting to note that the Ca distribution observed in frozen-hydrated 3T3 cells agrees with freeze-dried samples; however, the K levels in the nuclei seem slightly elevated (*9*). The effect of water matrix on these signals needs further consideration and is a subject of continued research in our group.

In summary, this preliminary study shows the potential of ion microscopy to perform analysis of frozen-hydrated biological specimens at cold temperatures. This study marks the beginning of future studies in assessing the definitive modes of sample preparation for studying the roles of diffusible ions in biological systems.

Registry No. H_2O^+, 56583-62-1; H_3O^+, 13968-08-6; potassium, 7440-09-7; calcium, 7440-70-2; sodium, 7440-23-5.

LITERATURE CITED

(1) Castaing, R.: Slodzian, G. *J. Microsc. (Paris)* **1962**, *1*, 395-410.
(2) Morrison, G. H.; Slodzian, G. *Anal. Chem.* **1975**, *47*, 932A-943A.
(3) Stika, K. M.; Bielat, K. L.; Morrison, G. H. *J. Microsc. (Oxford)* **1980**, *118*, 409-420.
(4) Chandra, S.; Morrison, G. H. In "Secondary Ion Mass Spectrometry SIMS IV"; Benninghoven, A., Okana, J., Shimizu, R., Werner, H. W., Eds.; Springer-Verlag: New York, 1984; pp 489-491.
(5) Ross, G. D.; Morrison, G. H.; Sacher, R. F.; Staples, R. C. *J. Microsc. (Oxford)* **1983**, *129*, 221-228.
(6) Bernius, M. T.; Chandra, S.; Morrison, G. H. *Rev. Sci. Instrum.* **1985**, *56*, 1347-1351.
(7) Chandra, S.; Morrison, G. H.; Wolcott, C. C., submitted for publication in *J. Cell Biol.*
(8) Chandra, S.; Morrison, G. H. *Science* **1985**, *228*, 1543-1544.
(9) Chandra, S.; Morrison, G. H.; Coulter, C. W.; Bloom, S. E. *J. Cell Biol.* **1984**, *99* (4) part 2, 424a.

Subhash Chandra
Mark T. Bernius
George H. Morrison*

Department of Chemistry
Cornell University
Ithaca, New York 14853-1301

RECEIVED for review August 5, 1985. Accepted October 24, 1985. This work was funded by the National Institutes of Health under Grant No. R01GM 24314.

Generalized Rank Annihilation Factor Analysis

Sir: The analytical chemist is frequently confronted with the problem of analyzing complex mixtures of which only concentrations of a few components are of interest. In these cases, it is desirable to be able to obtain quantitative information for the analytes of interest without concern for the rest of the components in the sample. Second-order bilinear sensors, i.e., sensors that yield a two-dimensional data matrix of the form $\mathbf{M}_{ij} = \sum_k \beta_k x_{ik} y_{jk}$, are specially suited for this purpose, and the preferred technique for quantitation is known as rank annihilation factor analysis, RAFA (*1*, *2*). So far this method has been applied to excitation–emission fluorescence (*1–3*), LC/UV (*4*), and TLC–reflectance imaging spectrophotometry (*5*) with good results. It is important to realize that not all two-dimensional techniques yield bilinear data arrays; e.g., 2D-NMR or MS/MS data in their raw forms are not bilinear.

A limitation of rank annihilation as originally formulated is that an iterative solution requiring many matrix diagonalizations is necessary (*1*). Lorber (*6*) has reported a noniterative solution presenting the problem as a generalized eigenvalue–eigenvector equation for which a direct solution is found by using the singular value decomposition. With his method, to obtain the concentrations of the p analytes of interest in the sample, its bilinear spectrum and the p calibration spectra for each pure analyte must be recorded to obtain the concentrations. Analysis for each analyte requires a separate calculation. This letter presents the generalized rank annihilation method, of which Lorber's noniterative method is a particular case, that allows simultaneous quantitation of analytes in a sample using just one bilinear calibration spectrum obtained from a mixture of standards, one standard for each analyte.

Generalized rank annihilation can determine the bilinear spectrum and the relative concentration for each analyte in the unknown mixture. The calculated spectra are next matched to those of the standards. It is then straightforward to determine the actual concentration of each analyte from its relative concentration and the concentration of the corresponding standard. The full bilinear spectrum of each analyte is not actually required for identification. One need only use a single order (e.g., only the UV spectrum in the LC/UV case) for the match. This is an unusual type of

0003-2700/86/0358-0496$01.50/0